



## Synthesis of indium tin oxide nanotubes using 2-methoxyethanol as solvent via simple template method

Haijiao Zhang<sup>a</sup>, Feng Ye<sup>a,\*</sup>, Limeng Liu<sup>a</sup>, Huifang Xu<sup>b</sup>, Chao Sun<sup>a</sup>

<sup>a</sup> School of Materials Science and Engineering, Harbin Institute of Technology, Harbin 150001, China

<sup>b</sup> School of Chemical Engineering and Technology, Harbin Institute of Technology, Harbin 150001, China

### ARTICLE INFO

#### Article history:

Received 8 February 2010

Received in revised form 14 May 2010

Accepted 21 May 2010

Available online 27 May 2010

#### Keywords:

Indium tin oxide

Nanotubes

2-Methoxyethanol

Metal-alkoxide

### ABSTRACT

Sn-doped In<sub>2</sub>O<sub>3</sub> [indium tin oxide (ITO)] nanotubes, about 250 nm in diameter and 2–5 μm in length, were prepared via a simple template method with 2-methoxyethanol as solvent. The hydrogen bond interaction between 2-methoxyethanol and the metal-alkoxide formed by reaction of metal ions with 2-methoxyethanol played an important role in fabricating intact ITO nanotubes. Additionally, the suitable concentration of 2-methoxyethanol (1–1.5 mol L<sup>-1</sup>) was necessary to prepare intact ITO nanotubes with smooth surfaces in this method. At room temperature, the synthesized ITO nanotubes exhibited strong PL emission at 473 nm, indicating a high level of oxygen deficiencies in the ITO nanotubes.

© 2010 Elsevier B.V. All rights reserved.

### 1. Introduction

Since the first report on the discovery of carbon nanotubes, various nanotubes with different compositions have been synthesized, such as TiO<sub>2</sub> [1], SnO<sub>2</sub> [2], V<sub>2</sub>O<sub>5</sub> [3], and ZnO [4], for the enhanced properties compared with their corresponding bulk materials. For instance, nanotubes have large inner volumes, which can be filled with various desired chemicals, biochemicals or gas species, ranging in size from small molecules to proteins [5,6]. Additionally, nanotubes have open channels, which makes the inner surface accessible and subsequent incorporation of species within the tubes particularly easy [7]. For synthesis of nanotubes, template-based strategies have mainly been applied for their simple processes using metal and organic crystals, the tobacco mosaic virus [8], and carbon nanotubes as templates. Especially, porous membranes have widely been used to prepare nanotubes. Typically, nanoporous anodized aluminum oxide (AAO) template is mostly used for the deposition of a variety of materials composed of metals, semiconductors, polymer, carbon [9–13] etc.

Indium tin oxide (ITO) as a transparent semiconductor has attracted intense interests because of its potential applications in fields of optoelectronic devices, flat-panel displays, organic light emitting diodes and solar cells [14–17]. However, the literatures

on ITO nanotubes are scarce by comparison with the large stack of works devoted to ITO films or nanowires [18,19]. It is therefore imagined that many current applications for ITO could be enhanced by synthesis of ITO nanotubes. For example, ITO nanotubes will find promising application in high-performance solid-state gas sensors due to their ultrahigh surface-to-volume ratio. But to present, the gas sensors are mainly focused on ITO thin films and nanowires, and seldom on ITO nanotubes due to their low productivity and imperfect structure, which limit their applications as high efficient materials for gas sensors. It is thus necessary to prepare intact ITO nanotubes through a simple method.

The sol–gel approach is an efficient solution-based method to deposit various ultrathin metal oxide films on substrate [20]. It is based on chemical adsorption of metal-alkoxide from covalently-bound monolayer, followed by hydrolysis to give a thin metal oxide gel film with hydroxylated surface for further film deposition. The film morphology can be controlled at the nanoscale level [21]. It is therefore applied widely in fabricating metal oxide nanotubes via sol–gel process in nanoporous templates. So, it is crucial to select a suitable solvent or metal-alkoxide in synthesizing intact ITO nanotubes. Such as, the precursors of indium methoxyethoxide (In(OCH<sub>2</sub>CH<sub>2</sub>OMe)<sub>3</sub> and tetraisopropoxytin–isopropanol adduct (Sn(O<sup>i</sup>Pr)<sub>4</sub>·<sup>i</sup>PrOH) were applied to prepare ITO nanotubes, which exhibited excellent electro-conductive character [18]. However, the multisteps reaction and expensive precursors limit the large scale production of ITO nanotubes, and therefore it is crucial to develop an alternative method to obtain ITO nanotubes efficiently.

In this study, the 2-methoxyethanol was used as solvent to synthesize ITO nanotubes by combining sol–gel process with the

\* Corresponding author at: School of Materials Science and Engineering, Harbin Institute of Technology, P.O. Box 433, Harbin, Heilongjiang Province 150001, China. Tel.: +86 451 86418736; fax: +86 451 86413922.

E-mail address: [yf306@hit.edu.cn](mailto:yf306@hit.edu.cn) (F. Ye).

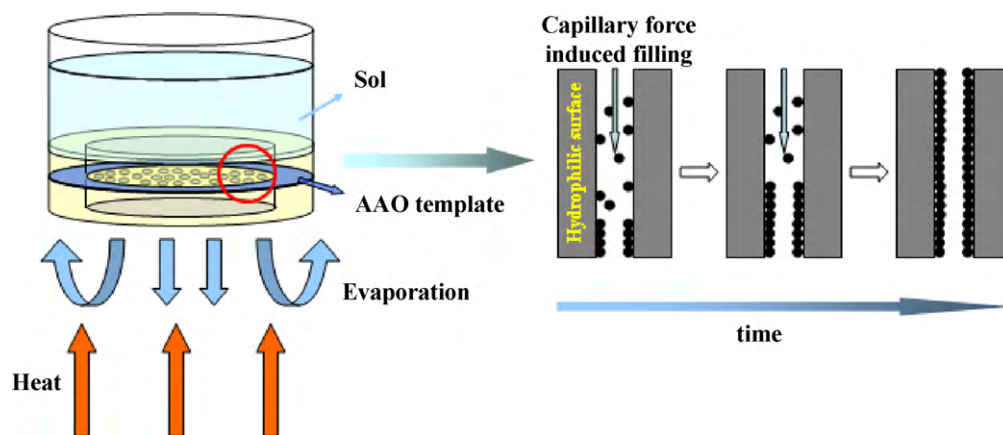


Fig. 1. The formation scheme of preparing intact ITO nanotubes using 2-methoxyethanol as solvent.

template technology based on porous AAO under mild conditions. The metal-alkoxides were formed via a simple sol–gel method. The hydrogen bonds between solvent of 2-methoxyethanol and metal-alkoxides played a crucial role in forming smooth and intact walls of ITO nanotubes. Finally, the PL properties of the ITO nanotubes were investigated.

## 2. Experimental details

### 2.1. Materials and preparation of ITO precursor

Nanoporous anodized aluminum oxide (AAO) template (Whatman International Ltd. Company, 50  $\mu\text{m}$ , 250 nm diameter pores) was heated at 500  $^{\circ}\text{C}$  for 3 h in vacuum, followed by boiling in 30 wt.%  $\text{H}_2\text{O}_2$  aqueous solution at 160  $^{\circ}\text{C}$  for 24 h to improve wettability. 0.78 g of indium nitrate pentahydrate ( $\text{In}(\text{NO}_3)_3 \cdot 5\text{H}_2\text{O}$ , 99.98%) and 0.0784 g of tin chloride ( $\text{SnCl}_4$ , 99.9%) were dissolved in 2-methoxyethanol

aqueous solution (0.5–2  $\text{mol L}^{-1}$ ), respectively, to obtain the individual solution. After the tin chloride solution was dropped into the indium nitrate solution, the solution mixture was refluxed at 80  $^{\circ}\text{C}$  for 24 h to be colorless and transparent, and then aged for 6–8 h at room temperature.

### 2.2. Synthesis of the ITO nanotubes

The treated AAO template was immersed and filled with the ITO precursor through the “down to up” method, as shown in Fig. 1. Firstly, the AAO template was fixed into a glass tube. Following that, the ITO composite precursor was dropped onto one side of AAO template. Simultaneously, the other side of AAO template was heated continuously at 40  $^{\circ}\text{C}$ . After several cycles, the immersing process of ITO mixed precursor was completed. Subsequently, the impregnated AAO template was heated at 80  $^{\circ}\text{C}$  for 48 h and then at 550  $^{\circ}\text{C}$  for 3 h in air. Finally, ITO nanotubes were collected by dissolving the AAO templates with a 1  $\text{mol L}^{-1}$  NaOH solution and centrifugation.

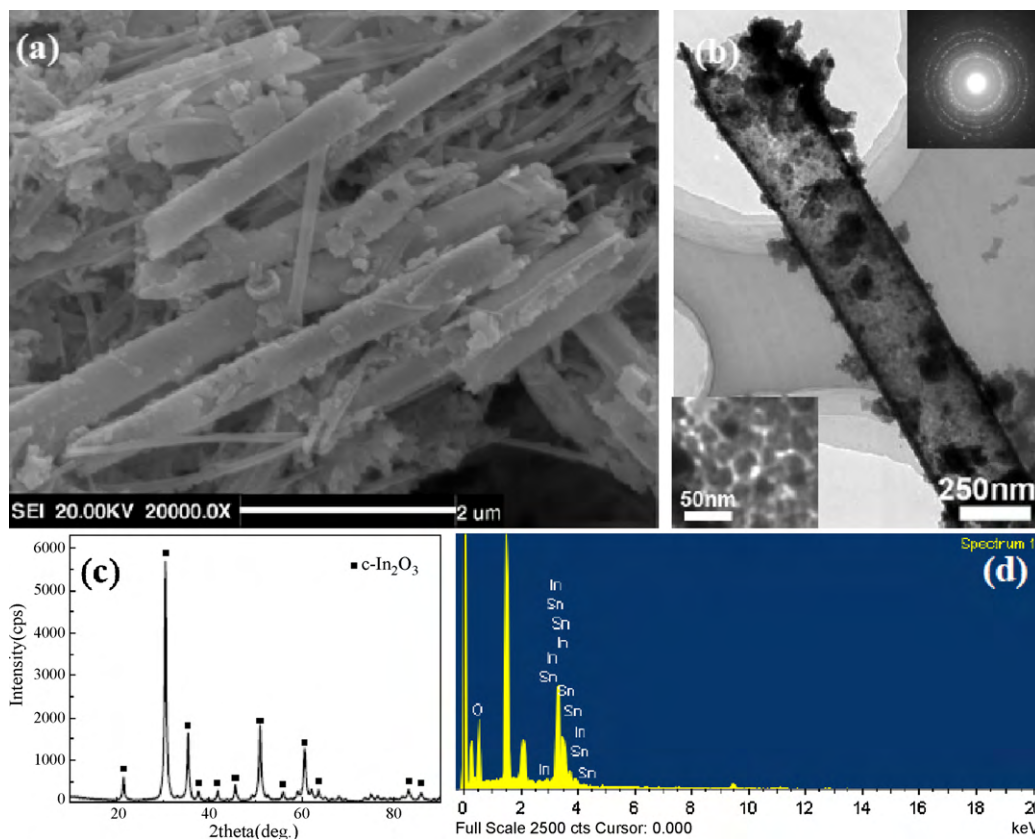


Fig. 2. The morphology and structure of the obtained ITO nanotubes: (a) SEM image, (b) TEM image, (c) XRD pattern, and (d) EDS spectrum.

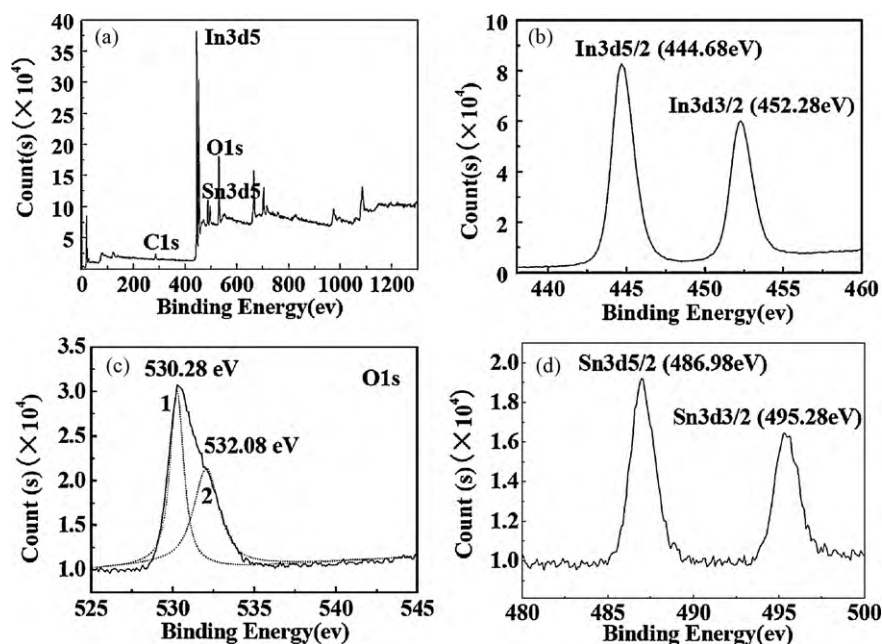


Fig. 3. XPS spectra of the prepared ITO nanotubes: (a) XPS wide scan, (b) narrow scan of In3d, (c) narrow scan of O1s, and (d) narrow scan of Sn3d.

### 2.3. Characterization

The microstructure and morphology of the ITO nanotubes were observed by scanning electronic microscopy (SEM, Jcxa-733) and transmission electronic microscopy (TEM, JEOLJEM-1200EX). Phase contents were determined by X-ray diffraction (XRD, Rigaku-D/max- $\gamma$ pc instrument) using Cu K $\alpha$  radiation. Chemical composition was investigated by energy-dispersive X-ray (EDX, model DX-4) fixed to the Jcxa-733. MK II X-ray photoelectron spectroscopy (XPS) instrument (employing Mg K $\alpha$ ) was further applied to study the composition of obtained ITO nanotubes. Photoluminescence (PL) excited by 250 nm using a 150 W Xe lamp was measured by a Hitachi F-4500 spectrofluorometer at room temperature.

## 3. Results and discussion

### 3.1. Morphology and crystal structure of ITO nanotubes

Typical SEM and TEM micrographs of the ITO nanotubes are shown in Fig. 2. Intact ITO nanotubes with diameter around 250 nm and length from 2 to 5  $\mu$ m were obtained using 2-methoxyethanol as solvent to prepare the precursor solution (Fig. 2a). The hollow structure of the ITO nanotubes composed of nanocrystals with

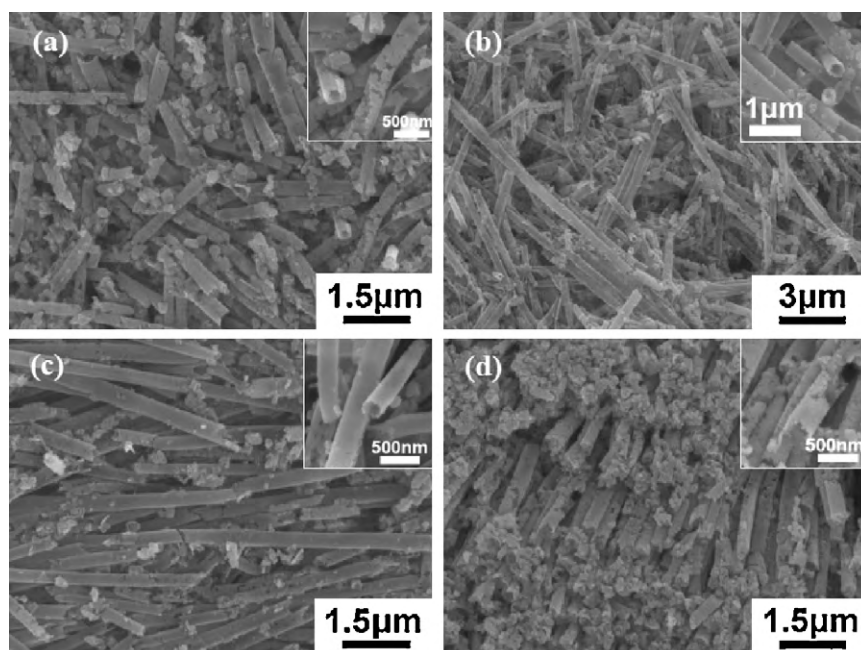


Fig. 4. SEM images of the ITO nanotubes prepared with different concentrations of 2-methoxyethanol: (a) 0.5 mol/L, (b) 1 mol/L, (c) 1.5 mol/L, and (d) 2 mol/L.

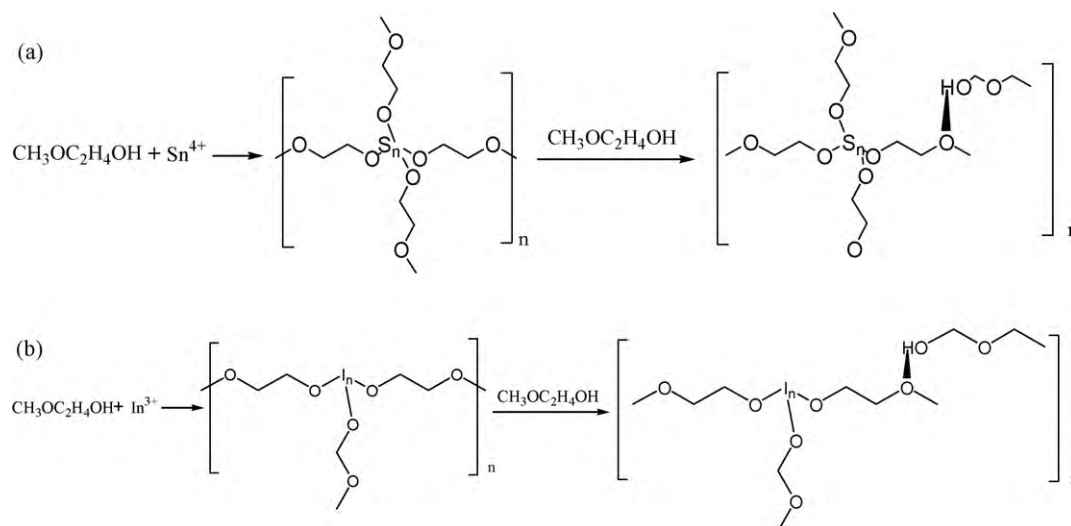


Fig. 5. Schematic illustrations of the formed metal-alkoxides: (a) Sn-alkoxide and (b) In-alkoxide.

diameter about 15 nm (insets of Fig. 2b) could be clearly observed by the TEM micrograph shown in Fig. 2b. The particles on the nanotube should be ITO pieces, which are also shown in the SEM micrograph in Fig. 2a. Fig. 2c shows the XRD pattern of the typical products. The sharp diffraction peaks suggest good crystallization. All the peaks can be indexed to a body-centered cubic  $\text{In}_2\text{O}_3$  (JCPDS 06-0416) with lattice constant  $a = 9.49 \text{ \AA}$ , which is smaller than the standard c- $\text{In}_2\text{O}_3$  ( $a = 10.11 \text{ \AA}$ ). Additionally, the Sn atomic radius (0.71 nm) is smaller than In atomic radius (0.81 nm), which will lead to the decrease of the planar spacing of  $\text{In}_2\text{O}_3$  crystal lattice. So, the XRD result indicates that the solid solution of Sn-doped  $\text{In}_2\text{O}_3$  was achieved, rather than a mixture of  $\text{In}_2\text{O}_3$  and  $\text{SnO}_2$  formed after the heat-treatment step. EDS shows  $\sim 10 \text{ mol\% Sn}^{4+}$  in respect to  $\text{In}^{3+}$  in the Sn-doped  $\text{In}_2\text{O}_3$  structure, which is consistent with the initial stoichiometric proportion (Fig. 2d).

XPS was used to further determine the composition of products. The wide XPS scan (Fig. 3a) clearly shows the photoelectron peaks of In, Sn, O, and C. The corresponding XPS spectra are  $\text{In}3d5$  (Fig. 3b),  $\text{O}1s$  (Fig. 3c), and  $\text{Sn}3d5$  (Fig. 3d). From Fig. 3b, the binding energy of  $\text{In}3d5/2$  is lowered slightly from 444.8 ( $\text{In}_2\text{O}_3$ ) to 444.68 eV. The spectrum (Fig. 3c) is deconvoluted into two peaks by the best fitting with Gaussian function. Peak 1 at 530.28 eV is due to the bulk  $\text{O}^{2-}$  ions. Indium atoms have a full complement of six nearest  $\text{O}^{2-}$  ions. Peak 2 at 532.08 eV is corresponded to the  $\text{O}^{2-}$  ions in oxygen

deficiency regions [22,23], which shows that oxygen deficiencies exist in ITO nanotubes. The binding energy of  $\text{Sn}3d5/2$  (Fig. 3d) at 486.98 eV is higher than that of tin oxide (486.4 eV). The spectra further indicate that atomic O is bonded to the  $\text{In}^{3+}$  and  $\text{Sn}^{4+}$  so that ITO was formed [24].

In preparation of intact ITO nanotubes, the 2-methoxyethanol revealed an optimum concentration, as shown in Fig. 4. In samples prepared with 0.5 and  $2 \text{ mol L}^{-1}$  2-methoxyethanol, ITO nanotubes with coarse surface were obtained (Fig. 4a, d, and insets). By comparison, in the samples with 1 and  $1.5 \text{ mol L}^{-1}$  2-methoxyethanol, it is found that the ITO nanotubes show smooth surface (Fig. 4b, c, and insets). The results indicate that the morphologies of final products are affected by the concentration of 2-methoxyethanol. At low concentration of 2-methoxyethanol, the rapid evaporation of 2-methoxyethanol would result in the aggregation of ITO gel particles. While, the high viscosity precursor formed at high concentration of 2-methoxyethanol will excessively stack in nanopores of AAO template, and finally ITO glomeration was produced. According to the previous works, the viscosity for 2-methoxyethanol exhibited a maximum when the molar concentration, between water and 2-methoxyethanol, was about  $11.57 \text{ mol L}^{-1}$  [25]. While, in this method, the mole fraction ( $0.5\text{--}2 \text{ mol L}^{-1}$ ) is lower than that of reported maximum, revealing a trend of increase in viscosity [25]. Therefore, the intact ITO

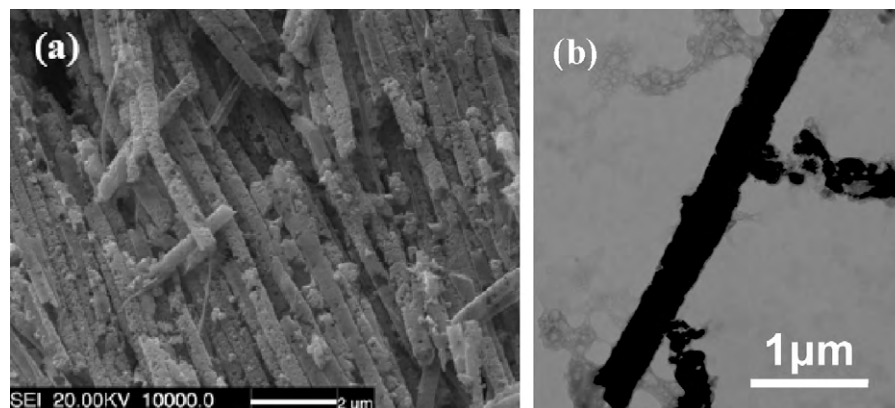


Fig. 6. SEM image (a) and TEM image (b) of the ITO nanorods prepared using 2,4-pentanedione as solvent.

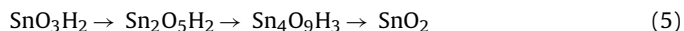
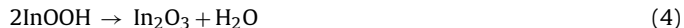
nanotubes with smooth surfaces would be generated in a suitable range (1–1.5 mol L<sup>-1</sup>) of concentration of 2-methoxyethanol in this approach.

### 3.2. Formation mechanism of the ITO nanotubes

The formation mechanism of the ITO nanotubes is speculated to be associated with the hydrolysis-co-precipitation reactions and dehydration of the In<sup>3+</sup> and Sn<sup>4+</sup> cations. This is because that the H<sub>2</sub>O in the solution and the hydrogen ions bonded to the oxygen atoms in the ethers of 2-methoxyethanol would lead to the complete hydrolysis of the In<sup>3+</sup> and Sn<sup>4+</sup> by Eqs. (1)–(3) [26,27]. Moreover, the 2-methoxyethanol solvent as a typical glycol-ether compound is important for the setup of the intact ITO nanotubes. According to the previous reports, the hydrolysis effects of the glycol from the 2-methoxyethanol promote the connection between metal-alkoxide and 2-methoxyethanol [28,29]. So, the hydrolysis reaction is balanced by glycol, resulting in the formation of uniform ITO thin films on the walls of AAO template.



Fig. 5 illustrates the build-up processes of the metal-alkoxide in the 2-methoxyethanol solvent. The 2-methoxyethanol is easy to form hydrogen bonds, as shown in Fig. 5a and b, by which uniform and stable thin film of the metallo-organic precursor on the inner walls of the porous AAO template can be formed [30]. The subsequent dehydration of the co-precipitates as shown by Eqs. (4) and (5) after a proper heat-treatment [27] results in the formation of ITO with perfect nanotube structure.



In contrast, ITO nanorods with rough surfaces were generated using 2,4-pentanedione as solvent (Fig. 6a and b), which hardly provides the crucial hydrogen bonds among chelate compounds. This is because that the indium ions located in the center of chelate compounds are surrounded by lots of hydrophobic alkyls. The hydrophobic colloidal particles repulse each other and stack randomly, inducing ITO precursor to nucleate and grow preferentially at defects of AAO template, and finally resulting in the rough and discrete structure of the ITO nanorods. Comparison between 2-methoxyethanol and 2,4-pentanedione solvents gives us a clear view of the important effects of the solvent on the self-assemble behavior of the ITO nanotubes.

### 3.3. Optical properties of the ITO nanotubes

The photoluminescence (PL) spectrum measured at room temperature of the typical intact ITO nanotubes, prepared at concentration of 1 mol L<sup>-1</sup> 2-methoxyethanol, is shown in Fig. 7. The PL peak at 505 nm is induced by scattering of the nanostructure. Strong PL emission centered at 473 nm is recorded, suggesting a high level of oxygen deficiencies in the ITO nanotubes [31]. It has been reported that the PL mechanism of In<sub>2</sub>O<sub>3</sub> matrix composite was mainly attributed to the effect of the oxygen deficiencies [32,33]. However, it is well known that ITO film cannot emit visible light even though it also contains oxygen deficiencies [34]. With respect to the prepared ITO nanotubes, firstly, the possibility of the observed PL arising from a quantum confinement effect is excluded, because the diameters of the ITO nanotubes seem too large to show a quantum confinement effect [35]. Secondly, the ITO nanotubes with high aspect ratio and peculiar morphology have

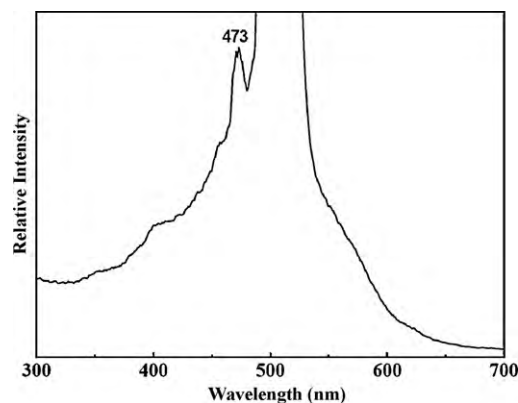


Fig. 7. Photoluminescence spectrum of the typical intact ITO nanotubes.

larger surface-to-volume ratio than that of the ITO films, which favors the existence of large quantities of oxygen vacancies. Thirdly, the high level of oxygen deficiencies should be associated with the free 2-methoxyethanol molecules which evaporated under the gel condition because of the weak hydrogen bonds [36]. In addition, in this study, during the heat-treatment process, oxygen vacancies could be generated on the surfaces of ITO nanotubes. So the strong emission at 473 nm of ITO nanotubes is likely related to surface oxygen vacancies and defects.

## 4. Conclusions

In this paper, a feasible method was reported to prepare intact ITO nanotubes with 2-methoxyethanol as solvent based on an improved template technology. It is decisive to use 2-methoxyethanol as solvent for forming intact ITO nanotubes due to the hydrogen bond interaction between the formed metal-alkoxides and 2-methoxyethanol. The prepared intact ITO nanotubes showed smooth surfaces compared to those of the ITO nanotubes reported in other literatures. Strong PL emission centered at 473 nm suggested a high level of oxygen deficiencies in the ITO nanotubes, indicating that the prepared ITO nanotubes are promising in application as laser materials.

## Acknowledgment

This work was supported by the Outstanding Young Foundation of Heilongjiang Province (JC200603).

## References

- [1] H. Yang, C.X. Pan, *J. Alloy Compd.* 492 (2010) 33–35.
- [2] J.F. Ye, H.J. Zhang, R. Yang, X.G. Li, L.M. Qi, *Small* 6 (2010) 296–306.
- [3] W. Jin, B. Dong, W. Chen, C. Zhao, L. Mai, Y. Dai, *Sens. Actuators B* 145 (2010) 211–215.
- [4] C.L. Cheng, J.S. Lin, Y.F. Chen, *J. Alloy Compd.* 476 (2009) 903–907.
- [5] R. Olive-Monllau, M.J. Esplandiú, J. Bartroli, *Sens. Actuators B* 146 (2010) 353–360.
- [6] J. Zhong, J.H. Guo, B. Gao, *Carbon* 48 (2010) 1970–1976.
- [7] C.R. Martin, P. Kohili, *Nat. Rev. Drug Discov.* 2 (2003) 29–37.
- [8] X.N. Wang, Z.W. Niu, S.Q. Li, Q. Wang, X.D. Li, *J. Biomed. Mater. Res.: A* 87A (2008) 8–14.
- [9] Z. Zhang, L.F. Liu, T. Shimizu, S. Senz, U. Gösele, *Nanotechnology* 21 (2010), 0556031–0556036.
- [10] G.O. Ince, G. Demirel, K.K. Gleason, M.C. Demirel, *Soft Mater.* 6 (2010) 1635–1639.
- [11] L.C. Liu, S.-H. Yoo, S.H. Park, *Chem. Mater.* 22 (2010) 2681–2684.
- [12] H.Y. Wu, Y. Zhao, Q.Z. Jiao, *J. Alloy Compd.* 487 (2009) 591–594.
- [13] G.P. Sklar, K. Paramguru, M. Misra, *Nanotechnology* 16 (2005) 1265–1271.
- [14] A.V. Moholkar, S.M. Pawar, K.Y. Rajpure, V. Ganesan, C.H. Bhosale, *J. Alloy Compd.* 464 (2008) 387–392.
- [15] W.-S. Cheong, Y. Yoon, J.-H. Shin, C.-S. Hwang, H.Y. Chu, *Thin Solid Films* 517 (2009) 4094–4099.
- [16] J.H. Park, J.H. Chae, D. Kim, *J. Alloy Compd.* 478 (2009) 330–333.

- [17] L. Kerkache, A. Layadi, A. Mosser, *J. Alloy Compd.* 485 (2009) 46–50.
- [18] Y. Aoki, J.G. Huang, T. Kunitake, *J. Mater. Chem.* 16 (2006) 292–297.
- [19] M.D. Dickey, E.A. Weiss, E.J. Smythe, R.C. Chiechi, F. Capasso, G.M. Whitesides, *ACS Nano* 2 (2008) 800–808.
- [20] C.-Y. Tsay, K.-S. Fan, S.-H. Chen, C.-H. Tsai, *J. Alloy Compd.* 495 (2010) 126–130.
- [21] Y. Aoki, T. Kunitake, *Adv. Mater.* 16 (2004) 118–123.
- [22] H. Yumoto, T. Sako, Y. Gotoh, K. Nishiyama, T. Kaneko, *J. Cryst. Growth* 203 (1999) 136–140.
- [23] G. Frank, L. Brock, H.D. Bausen, *J. Cryst. Growth* 36 (1976) 179–180.
- [24] S.S. Kim, S.Y. Choi, C.G. Park, H. Woo Jin, *Thin Solid Films* 347 (1999) 155–160.
- [25] M.N. Islam, M.M. Islam, M.N. Yeasmin, *J. Chem. Thermodyn.* 36 (2004) 889–893.
- [26] D. Yu, D. Wang, Y. Qian, *Inorg. Chem. Commun.* 5 (2002) 475–477.
- [27] H. Yang, S. Han, L. Wang, I.J. Kim, Y. Son, *Mater. Chem. Phys.* 56 (1998) 153–156.
- [28] W. Sakamoto, Y. Masuda, T. Yogo, *J. Alloy Compd.* 408–412 (2006) 543–546.
- [29] H. Liu, J. Xie, K. Wang, *J. Alloy Compd.* 459 (2008) 521–525.
- [30] W. Sakamoto, T. Yogo, K. Kikuta, T. Arimoto, S. Hirano, *J. Am. Ceram. Soc.* 79 (1996) 889–894.
- [31] B.M. Quinn, C. Dekker, S.G. Lemay, *J. Am. Chem. Soc.* 127 (2005) 6146–6147.
- [32] L.X. Zhang, Y.C. Zhang, M. Zhang, *Mater. Lett.* 64 (2010) 966–968.
- [33] F. Yang, J. Ma, X. Feng, L. Kong, *J. Cryst. Growth* 310 (2008) 4054–4057.
- [34] Q. Wan, Z.T. Song, S.L. Feng, T.H. Wang, *Appl. Phys. Lett.* 85 (2004) 4759–4761.
- [35] C. Liang, G. Meng, Y. Lei, F. Phillipp, L. Zhang, *Adv. Mater.* 17 (2001) 1330–1334.
- [36] R.L. Brinkley, R.B. Gupta, *Ind. Eng. Chem. Res.* 37 (1998) 4823–4827.